

# The use of Global Positioning System techniques for the continuous monitoring of landslides: application to the Super-Sauze earthflow (Alpes-de-Haute-Provence, France)

J.-P. Malet<sup>a,\*</sup>, O. Maquaire<sup>a</sup>, E. Calais<sup>b</sup>

<sup>a</sup>*Centre d'Etudes et de Recherches Eco-Géographiques, UMR-7007 CNRS-ULP-ENGEEES, 3, rue de l'Argonne, F-67083 Strasbourg Cedex, France*

<sup>b</sup>*Géosciences Azur, UMR 6526-CNRS, 205, rue Albert Einstein, F-06560 Valbonne, France*

Received 4 August 2000; received in revised form 31 January 2001; accepted 3 June 2001

---

## Abstract

Recent researches have demonstrated the applicability of using *Global Positioning System* (GPS) techniques to precisely determine the 3-D coordinates of moving points in the field of natural hazards. Indeed, the detailed analysis of the motion of a landslide, in particular for a near real-time warning system, requires the combination of accurate positioning in three dimensions (infracentimetric) and fine temporal resolution (hourly or less). The monitoring of landslides with the GPS is usually performed using repeated campaigns, as a complement to conventional geodetic methods. Continuous monitoring of landslides with GPS is usually not performed operationally, mostly because of the cost of such a system compared to conventional deformation monitoring techniques. In addition, if GPS measurements can reach a millimetre-level accuracy for long observation sessions (typically 24 h), their accuracy decreases with the duration of the observation sessions, because of errors introduced by variations of the satellite constellation and multipath effects at the sites. This study aims at determining the experimental accuracy of GPS measurements for the continuous monitoring of landslides with GPS. In particular, we want to calibrate the variation of the measurement accuracy as a function of the duration of the observation sessions. The study was carried out on the Super-Sauze earthflow (Southern Alps, France) which evolves in a channelized flow with surface displacements reaching a few tens of centimetres to a few metres per year. The GPS data were acquired during two campaigns in May and October 1999 (two reference stations were installed outside the flow and four “moving” stations distributed on the flow). The maximal 3-D cumulative displacement reaches 2.1 m during 3 weeks in May 1999. The accuracy for a 1-h session reaches 2.7, 2.2 and 5.0 mm for the north–south, east–west and vertical components, respectively. The detectability threshold for a significant motion and a given temporal resolution stands between 3.5 mm/24 h and 8.5 mm/h in planimetry, between 6 mm/24 h and 19.5 mm/h in altimetry. Thus, the motion of the flow is clearly detected by the GPS measurements and the results have been compared with those obtained with conventional geodetic methods (theodolite and electronic distance-meters) or with a wire extensometer device. In addition, combination of periodical topometric measurements, continuous extensometric and GPS measurements allows us to identify seasonal and episodic transient variations in the surficial velocity of the flow. The analysis of the relationships between rainfall (and snowfall), groundwater level, and displacements permits us to understand the behaviour of the flow and to determine pore water pressures (PWP) thresholds initiating an acceleration of the movement. GPS therefore appears applicable to the

---

\* Corresponding author.

E-mail address: malet@equinox.u-strasbg.fr (J.-P. Malet).

continuous monitoring of geophysical objects or of man-made structures with small and slow displacements ( $\sim 5$  mm/day). This technique does not require direct line of sight between the “moving” sites and the reference stations. Measurements can be carried out in all weather and at night. GPS processing can be performed in near real time without loss of accuracy. The use of GPS is, however, limited by the environmental characteristics of the geophysical object (mountains, vegetation), which can constitute masks limiting the visibility of the sky and create multipaths effects. © 2002 Elsevier Science B.V. All rights reserved.

*Keywords:* GPS; Millimetric positioning; Continuous monitoring; Earthflow; Geodesy; Landslides

## 1. Introduction

Techniques of positioning on various time and space scales have made a lot of progress in the last decade, in particular in the field of geomorphological mapping, or in the realization of Digital Elevation Model (DEM) by numerical photogrammetry (Girault, 1992; Miyazawa et al., 2000; Weber and Herrmann, 2000), radar interferometry (Fruneau et al., 1996; Mohr et al., 1998; Singhroy, 1998; Kimura and Yamaguchi, 2000) or by *Global Positioning System* (Fix and Burt, 1995; Higgitt and Warburton, 1999). These new technologies present attractive and quick solutions, usable in any type of morphological configuration and provide data easily integrable in a Geographical Information System (GIS) format, with resolutions between tens of metres to centimetres. If these methods are today commonly adopted for mapping, less attention has been paid to the potential use of these techniques, and in particular to GPS, for the continuous monitoring of geophysical entities such as landslides or man-made works. Any surveying network must provide reliable information on the evolution of the phenomenon to the responsible authorities, which may have to take quick decisions for the safety or the evacuation of people and property. Therefore, this information will have to be transmitted in near real time to a decision center and should be easily interpretable.

After providing an overview of the main methods applied to the survey and the monitoring of landslides, and using the Super-Sauze earthflow as an example, this article has the following objectives:

(i) to demonstrate the difficulties for the establishment and the conservation of “traditional” displacement surveying network by point topometric

measurements and continuously by a wire extensometer;

(ii) to provide useful information on the respective accuracy of these techniques, taking into account the precautions of implementation, use and operating modes;

(iii) to evaluate quantitatively the contribution of continuous GPS for the fast detection of small displacements.

To evaluate the potential of GPS measurements to combine spatial accuracy and temporal resolution, a methodological study was carried out with the aim of determining the experimental accuracy which is possible to reach while calibrating, in particular the variation of the accuracy as a function of the duration of the observation sessions. A number of studies of the statistical properties of GPS measurements have shown that the formal error derived from the inversion of phase data underestimates the true measurement accuracy by a factor ranging up to 11 (Zhang et al., 1997; Mao et al., 1999).

The GPS results are compared with the results obtained by topometry and extensometry measurements. These results lead to the determination of optimal processing strategies and argue the advantages and disadvantages of GPS measurements for continuous monitoring, with the aim of considering a device adapted to a near real time warning system. The results of this study are applicable to the continuous monitoring of the deformation of active volcanoes or of man-made works. Moreover, the detailed analysis of the 3-D ground displacements in relation to hydroclimatic conditions makes it possible to release first results on the complex conditions and rates of behaviour of the Super Sauze earthflow.

## 2. Methods and techniques for the monitoring of landslides

It is useful to recall, although not in an exhaustive and historical manner, the methods, techniques and operating modes applied to landslide monitoring and the technical progress accomplished in this field for two decades. All around the world, several unstable sites are instrumented according to devices adapted to the intensity of the phenomena considered (rockfalls, cliff collapses, debris flows, earthflows) and to the induced risks. In France, examples are the La Clapière landslide (Follacci, 1999), the Ruines de Séchilienne landslide (Rochet, 1992), the La Valette earthflow (Colas and Locat, 1993), and on the southern coast of England, an example is the St. Catherine's Point landslide (Bromhead et al., 1988). Morphological mapping and the survey of ground movements can be carried out in two ways according to the scale considered. The first consists of analysing and comparing various types of documents (topographic maps, aerial photographs, cadastral maps, DEMs) which represent instantaneous views of an unstable site on various dates. It enables to reconstitute the historical development of the phenomenon on scales ranging from the 1:10 000 to the 1:1000 (EPFL, 1985a; Engel,

1986; Maquaire, 1990; Martin and Weber, 1996; Powers and Chiarle, 1996).

The second consists in carrying out in situ measurements of the surficial displacements by combining a space and time resolution adapted to the evolution speeds of the phenomena.

Within this framework, a large variety of techniques has been used (Table 1) to follow the movements of unstable slopes (Krauter, 1988; LCPC, 1994a; Mikkelsen, 1996). Fissurometers or short-base extensometers have been used to record the distance variations between "moving" points or the opening of cracks on rock escarpments (Gulla et al., 1988; Evrard et al., 1990) or on man-made structures (LCPC, 1994b). Tacheometric levels, theodolites, distance-meters and geodetic stations make it possible to measure continuous slope displacements by the survey of "moving" targets. Terrestrial or air stereophotogrammetry provides the 3-D coordinates of "moving" points and leads to the realization of morphological maps and especially the generation of DEMs and cross-sections along the unstable slope (Oka, 1988; Weber and Herrmann, 2000). Conventional geodetic techniques (triangulation, tacheometry) and extensometry techniques (Angeli et al., 2000) remain to be the most commonly used because it is

Table 1

Overview and characteristics of the main methods in monitoring surficial displacements and their precision (EPFL, 1985a; LCPC, 1994a; Gili et al., 2000)

Method	Use	Results	Typical range	Typical accuracy
Micrometer screw-level	Angular displacement	$d\alpha$	0.1 rad	$4.10^{-4}$ rad
Fissurometer	Differential movement of compartments	$dD$	<20 mm	$\pm 0.1$ mm
Levelling vernier pole	Opening of small cracks	$dD$	<200 mm	$\pm 0.5$ mm
Short-base extensometer	Opening of cracks	$dD$	25–450 mm	$\pm 0.1$ mm
Invar distance-meter	Displacements of moving targets	$dD$	Up to 40 m	$\pm 0.1$ mm
Wire extensometer	Displacements of moving targets	$dD$	Up to 100 m	$\pm 0.5$ mm
Tacheometric level	Variation of altitude	$dZ$	Variable	20 mm
Electrooptic distance-meter	Displacements of moving targets	$dD$	1–10 km	7 mm $\pm 1-5$ ppm
Geodetic station	Displacements of moving targets	$dX, dY, dZ$	1–10 km	3 mm $\pm 1-5$ ppm
GPS	Displacements of moving targets	$dX, dY, dZ$	Baseline <20 km	1–2 mm
Terrestrial photogrammetry	Displacements of moving targets	$dX, dY, dZ$	<200 m	40 mm
Aerial photogrammetry	Displacements of moving targets DEM comparison	$dX, dY, dZ$	$H_{flight} < 500$ m	100 mm
Radar interferometry INSAR <sup>a</sup>	DEM comparison	$dX, dY, dZ$	Variable	3–5 mm
DORIS <sup>b</sup>	Displacements of moving targets	$dX, dY, dZ$	Variable	2 mm

<sup>a</sup> Interferometric Synthetic Aperture Radar.

<sup>b</sup> Détermination d'Orbites et Radio-Positionnement Intégrés par Satellite.

possible to reach an accuracy of a few millimetres on short baselines of less than a kilometre.

The Global Positioning System (GPS) is a satellite positioning technique used largely in geophysical research, in particular for the measurement of active crustal deformations (Dixon, 1991). The use of the phase measurements makes it possible to determine the relative positions of points located as far as several hundred kilometres apart with an accuracy of 1–2 mm in planimetry and 5–10 mm in altimetry. This accuracy allows the fast detection of weak displacements and, thus, the survey of the temporal evolution of natural hazards (volcanoes, tectonic faults and landslides). The GPS equipment has become progressively less expensive, lighter and easier to use. New operating modes, methodologies and software have been developed for the data recording and post-processing. GPS is thus increasingly used in a large variety of applications, such as establishment of control points for photogrammetry or remote-sensing applications, positioning of drillings, coastline evolution, or DEM generation.

In the field of surveying, GPS precise applications were progressively conceived and developed in the early 1980s. The positioning of the Positron of the CERN (European organization for nuclear research) was checked by GPS (Gervaise et al., 1985) with an error of  $\pm 4$  mm for baselines from 3 to 13 km. For the monitoring of crustal deformations, Larson and Agnew (1991) or Peler et al. (1998) reach an accuracy of  $\pm 2$  mm on 2 km-baselines. In the field of the environment, GPS was used: to follow the movements of spoil heaps or of quarry faces (Joass, 1993); to survey active volcanoes (Pingue et al., 1998; Mattioli et al., 1998; Sheperd et al., 1998) or major tectonic faults (Newmann et al., 1999); to monitor the flow and the behaviour of glaciers (Sjoberg et al., 2000) or snow thickness (Theakstone et al., 1999). The technique also applies, with a sufficient accuracy, to the monitoring of man-made structures, such as dams (Brown et al., 1999; Hudnut and Behr, 1998), bridges or viaducts.

For the monitoring of landslides, where the degree of accuracy required is millimetric, GPS has been used only for repeated measurements (Jackson et al., 1996; Hiura et al., 1996; Barbarella et al., 1998; Gili et al., 2000) as a complement to conventional geodetic methods. On the other hand, continuous monitoring of landslides with GPS is not usually performed operationally, mostly because of the cost of such a system

compared to conventional deformation monitoring techniques. In addition, if GPS measurements can reach a millimetre-level of accuracy for long observation sessions (typically 24 h), their accuracy decreases with the duration of the observation sessions, because of errors introduced by variations of the satellite constellation and multipath effects at the sites (Genrich and Bock, 1992). However, to analyse in detail landslide kinematics to model the evolution and the behaviour of these phenomena, especially if the monitoring is included in a near real-time warning system, it is necessary to obtain a precise 3-D position (millimetric) and a fine temporal resolution (hourly or infrahourly). Moreover, 1 mm-level accuracy requires sophisticated a posteriori data processing.

For all these reasons, the traditional methods of topometry (automated or not), which make it possible to reach precise details of a few millimetres on short baselines ( $< 1$  km) with fine temporal resolution (for instance, every 10 min at the La Clapière landslide; Follacci, 1999), still remain very competitive in particularly favourable sites. On the other hand, it will be shown in this article that for very constraining sites (accessibility, long-term stability of the slopes around the landslide, visibility) GPS now seems the only solution to obtain point or continuous reliable measurements on several points of the unstable area.

### **3. A very constraining study site: the Super-Sauze earthflow (Alpes-de-Haute-Provence, France)**

#### *3.1. Historical and morphological context*

The Super-Sauze earthflow (basin of Barcelonnette, Alpes-de-Haute-Provence, southeastern France) developed in an enclosed marly torrential basin (Callovo–Oxfordian black marls) gullied by badlands. It has an elevation between 2105 (crown) and 1740 m (toe of the flow) for a  $25^\circ$  slope, over a 17-ha area (Fig. 1a–c). Falls of blocks and structural slides of large slabs occurred in the 1960s (Malet et al., 2000), and the flow developed through the 1970s burying a stream channel (Fig. 1). This period marked the beginning of a generalised movement of the whole slope and the downstream progression (reconstituted by multirate photo-interpretation 1956/1995; Weber

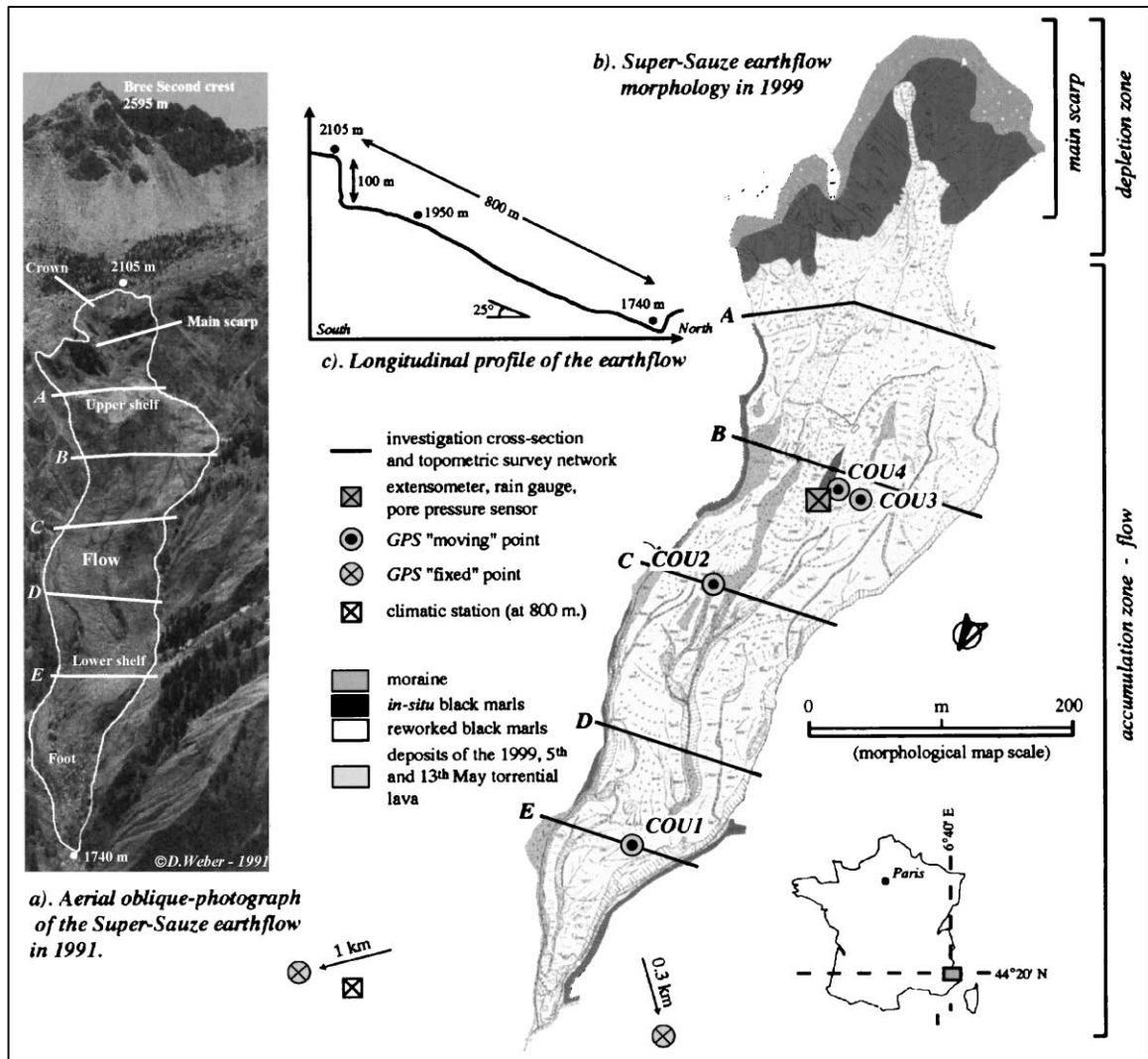


Fig. 1. Morphology, investigation and monitoring of the Super-Sauze earthflow (Alpes-de-Haute-Provence, southeastern France).

and Herrmann, 2000) of the toe by more than 180 m since 1982 (Flageollet et al., 1998). Geotechnical investigations, measurements of in-depth displacements by inclinometers (Flageollet et al., 2000) and geophysical prospecting (Schmutz et al., 1999) indicate that the flow buries an intact paleotopography (Flageollet et al., 2000) formed by a succession of parallel crests and gullies (Figs. 1a and 6). This paleotopography plays an essential role in the behaviour of the flow by delimiting preferential water and material pathways and compartments with different kinematic, mechanical and hydrodynamical character-

istics (Fig. 7b). The flow is structured in two vertical units (Fig. 7c) composed of weathered marly blocks, which divide downstream into smaller clasts and progressively feed the flow with fine-textured material (Klotz, 1999) of a clayey-marly matrix with clasts of all sizes, which corresponds to debris-flow deposits.

### 3.2. The surveying network

In order to determine the flow dynamics and to validate propagation models, a survey network was built up. The first point measurements of the surficial

displacement were carried out by topometry in 1991, in order to follow the withdrawal of the main scarp and the downstream progression of the flow (Weber, 2001). Since 1996, after modifications and additions, the network consists of about 70 targets distributed in five cross-sections (Fig. 1b). The hydroclimatic conditions which control the behaviour of the moving mass are continuously recorded by a water balance station, piezometers, raingauges and a meteorological station located at 1.4 km from the flow. The surficial velocity reaches, according to the location, a few centimetres to a few meters per year (Flageollet et al., 2000). If 8–10 topometric surveys are carried out each year between May and November (the flow is covered by snow during the winter), it quickly appeared essential to have continuous displacement measurements to define the complex relationship between these various parameters, and in particular, to check the influence of abrupt groundwater table (GWT) increase on the flow behaviour. With this intention (since June 1999), displacements are monitored continuously in the most active part of the flow (B cross-section) by a long base wire-extensometer (Angeli et al., 2000). Lastly, considering the variable velocity of the flow and that it was not possible to install an automated geodetic station to follow many targets or to install several extensometers (see Section 4.2), we installed several GPS antennas over a maximum continuous period of 20 days. The results from all of these devices will now be presented and analysed, while detailing the reasons for the choices on the basis of permanent and seasonal constraints.

## 4. Monitoring by topometry and extensometry

### 4.1. The topometric or geodetic positioning

#### 4.1.1. Principles, methodology and precautions

The establishment of the network has taken into account the experience gained over several years by various authors on many monitored sites for periodic surveys (Miserez, 1984; EPFL, 1985a; Bromhead et al., 1988; Varnes et al., 1996; Van Beurden, 1997) or for continuous survey with an automated geodetic station (Follacci, 1999; Rochet, 1992). Four essential aspects must be borne in mind when designing a surveying network: the degree of accuracy required,

the geomorphodynamic characteristics of the moving mass, the various site constraints and, lastly, the resources available for the operation. Topometry consists in determining the 3-D position of a point in space from angle and distance measurements made by optical sightings using a theodolite and an EDM. The most modern equipment can determine horizontal and vertical angles to within a decimilligrade (a displacement of 1.57 mm for a 100-m distant point) and oblique distance within a millimetre (standard deviation 3–4 mm + 1 ppm with atmospheric corrections). Theoretically, the accuracy obtained is better than 5 mm after taking into account certain precautions (quality of the theodolite position in the three dimensions, assessing the error of eccentricity by systematic double reversal procedures, calculating the atmospheric correction factor, avoidance of parallax errors by making two or three pointings, closing a round of angles, etc.; EPFL, 1985a; Maquaire and Levoy, 1987).

Laying out a survey network operational for several years, and in particular locating the “fixed” monitoring stations, leads to anticipating: the potential changes the site will undergo in the future (man-made works, vegetation growth, earth movements, etc.), the potential extension of the landslide, the long-term stability of the slope where the observation sites are located. Concrete pillars with centering plates guarantee an increased accuracy in three dimensions by preventing any errors of eccentricity during a survey lasting several hours and by facilitating the vertical positioning and the horizontal trimming of the apparatus. If the site allows good visibility of all the targets and if the measured distances are lower than 1.5 km, the suitable method of calculation is triangulation (Ashkenazi, 1973), which permits, with at least two survey stations, to define an ellipse of errors on the positioning of a point—the most probable position (known as the “corrected” point) is then calculated by compensation.

#### 4.1.2. Intrinsic accuracy of the Super-Sauze network

The network was surveyed from two concrete fixed pillars, PIL1 and PIL2, with centering plates, located on a narrow slope facing the earthflow, the only “stable” place in the catchment (Fig. 2a,b). This topographic constraint forced us to locate the two survey stations close to one another (only 70 m). This partly reduces the advantage of triangulation because of a very poor intersection angle between

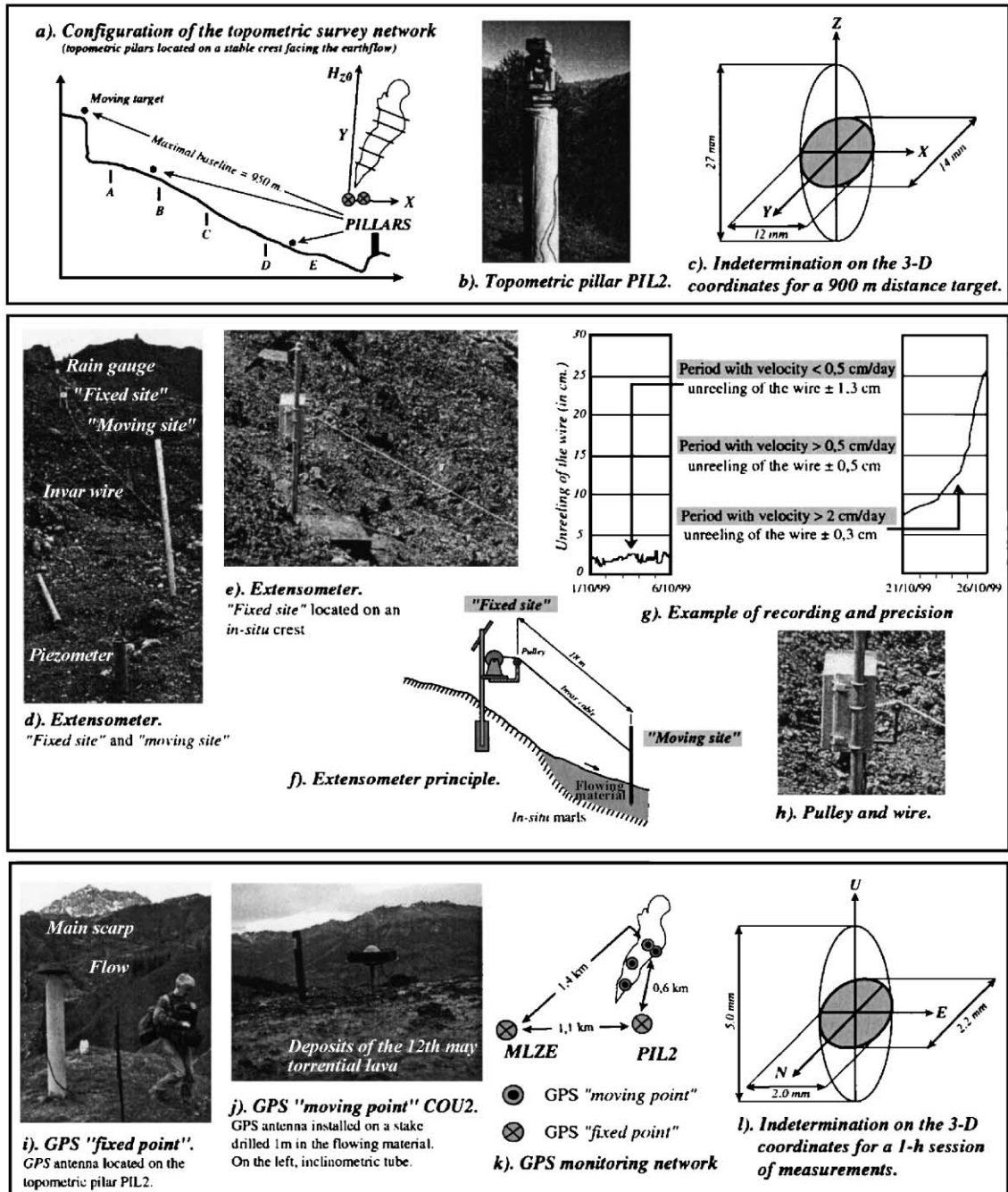


Fig. 2. Surveying methods of the Super-Sauze flow kinematics—topometric network and device (a), extensometric device (b), GPS device (c)—and respective precision.

the pointings made from the two pillars. The orientation of the horizontal circle was done by sighting a relay pylon at an altitude of 2150 m about 1.5 km from the survey stations. The pointing is carried out on a reflector mounted on a pole successively moved on each target localised in the field by discrete wooden or metallic stakes. The maximum measured distances reach 1 km for a maximum difference in level of 300 m. The accuracy for the targets located in the upper part of the flow and on the crown at 900 m reaches  $\pm 1.3$  cm in planimetry and  $\pm 2.7$  cm in altimetry (Fig. 2c; Flageollet et al., 1998). Accuracy increases for the targets located in the lower part of the flow as the distance to the observation pillars decreases. Since the end of 1997, because of the proven instability of the pillar PIL1, the network is only surveyed from site PIL2. However, it now appears that since 1999 (with the GPS measurements carried out), the stability of this latter pillar is no longer completely assured. This major constraint encouraged us to quickly find and adapt another reliable and perennial monitoring network.

#### 4.2. *The measurement of the surficial displacements by extensometry*

##### 4.2.1. *Principle of extensometry*

To measure continuous deformation of a geophysical object, a simple method consists of connecting one or more “moving” points to some “fixed” reference points, and to record the variations of these connections through time (EPFL, 1985b; Engel, 1986; Angeli et al., 2000). Adapted to natural phenomena, the method consists of connecting by a wire two points from the unstable slope. The measured deformations which correspond to the unreeling of the wire are absolute or relative, according to whether only one or the two points of the device move.

This principle was applied in the 1930s to the study of movements along tectonic faults or to the survey of the creep of glaciers (Röthlisberger and Aellen, 1970). It was only in the 1980s that this technique was applied to landslides, with an accuracy not exceeding 2–3 cm (Schlemmer, 1982; Brunsden and Prior, 1984; Sassa, 1984), then less than 1 cm (Engel, 1986; Angeli et al., 1995). The first devices used a revolving cylinder for the recording with all the inherent problems (pen, paper unfolding and examination). The

modern systems (potentiometric wheel connected to a datalogger) make it possible to be freed from this type of error and offer a greater degree of accuracy.

##### 4.2.2. *Equipment and intrinsic precision of the extensometric device*

The device consists of a “fixed” site and a “moving” site (Fig. 2d,e). The former is anchored on the only stable area of the flow, an in situ marly crest emerging from the flow, the stability of which has been measured and checked since 1996. The sensor has been assembled on a metal frame adjustable in height anchored deeply in the in situ marl by a concrete block (Fig. 2e,f). The detection of movement includes a potentiometric wheel, which measures the unreeling of the wire, a guiding pulley, which allows the perfect alignment of the wire between the sensor, and the “moving” point (Fig. 2h). The wire is in invar (i.e. low thermal expansion). The tension of the wire is held up by a system of brakes integrated into the potentiometric device. The unreeling of the wire, the air temperature and the rainfall were recorded by a datalogger (Campbell CR10X) every 6 min. The “moving” site is a metal stake drilled 2 m into the flowing marly material. The unrolled length (18–20 m) generates a rise of about 15 cm under the weight of the wire.

The precision of the device is proportional to the unrolled length of the wire, taking into account the effects of the wind, which cause the wire to vibrate, the possible formation of ice on the wire, the thermal dilation of the wire (very reduced in our case by the use of an invar wire), the fortuitous passage of game, etc. The effect of the wind was mitigated, on the one hand, by installing the cable as near as possible to the ground, and on the other hand, during the post-processing of the “signal” by smoothing the data with a moving average filter. As shown in Fig. 2g, the effect of the wind is insignificant if the velocity is important.

Check measurements are regularly taken (topometry, measurements of the wire’s length and of the wire’s rise). The displacement vectors are calculated by taking account of the slope and the rise of the wire, which varies progressively during the unreeling. After calibration of the system in the laboratory, taking into account the rise, comparison of the “calculated” displacements to those measured by topometry, the

“field” accuracy reaches  $\pm 3$  mm when the velocity of the flowing material is higher than 2 cm/day and  $\pm 13$  mm when the velocity falls under 0.5 cm/day (Fig. 2g).

## 5. The Global Positioning System

### 5.1. Principle of the positioning

We present here only the basic principles necessary for the comprehension of the GPS operating mode. The bases of the GPS technique (principle, applicability, procedures of measurements, equipment, accuracy) are described by several authors (Leick, 1995; Herring, 1996; Hofmann-Wellenhof et al., 1997). The GPS is a radionavigation, timing and positioning system based on a constellation of 26 satellites in orbit around the earth at altitudes of approximately 20 000 km. These satellites emit continuous electromagnetic waves coded on two frequencies ( $L1 = 1.2$  GHz and  $L2 = 1.5$  GHz). If the positions of the satellites on their orbits are precisely known and if the antenna collects at least four satellites, the receiver can solve by trilateration the three unknown factors defining its position.

The accuracy of the positioning will depend, on the one hand, on the quantity of information that a receiver is able to decode (code and phase measurements, mono- or dual-frequency receiver); and on the other hand, on the strategy used to calculate the position (Hofmann-Wellenhof et al., 1997). Indeed, a precise positioning requires a very precise measurement of time. As a consequence, a few millimetres accuracy positioning is only possible in slightly differed time, by processing the data a posteriori by complex algorithms, taking into account all potential errors.

Let us quote in particular the influence of the ionosphere and troposphere which slow down the propagation of the GPS signal or the precise knowledge of the satellites' orbits (Dixon, 1991). Moreover, it is necessary to be situated in relation to one or more “fixed” stations (base) located on a point whose position is well known. This differential mode of acquisition (DGPS) makes it possible to be freed from certain systematic errors (atmospheric delays, precision of the orbits, ephemerides, selective availability) which will be identical for all the antennas.

Lastly, the use of adapted antennas and their installation on open sites must limit the multipath effects, additional errors introduced in the resolution of the equations (Gili et al., 2000).

### 5.2. Methodology and equipment

The GPS data were acquired using six dual-frequency Ashtech Z-XII receivers equipped with Choke-Ring antennas limiting the multipaths during two campaigns, from May 7 to 23, 1999 and from October 9 to 15, 1999. In May 1999, two reference stations were installed outside the flow: MLZE on the roof of a small building of the Super-Sauze ski station and PIL2 on the tacheometric pillar PIL2 (Figs. 1a and 2b,k). Four “moving” stations were distributed on the flow in areas with a different kinematic behaviour (COU1 to COU4; Figs. 1a and 2i–k). GPS antennas were installed on a PVC tube drilled 1.5 m in the flowing material (Fig. 2j). In October 1999, only two receivers were used. A reference site was installed outside the flow on a site occupied in May (MLZE), another on the flow in the vicinity of site COU4.

The maximum length of the baselines reaches 1.4 km, the maximal difference in level is 200 m. The GPS data were sampled at 30-s intervals with a  $10^\circ$  cut-off angle and a minimum of one satellite visible. The receivers were supplied by solar panels. The lack of insolation during the first half of the May 1999 campaign caused several breaks in the recordings. Moreover, several topometric checks were undertaken in parallel during the two campaigns.

GPS code and phase measurements were processed in static mode with the GAMIT software (King and Bock, 1995). First, the precise coordinates of the bases (MLZE and PIL2) were calculated in the ITRF96 geodetic reference network. On a second occasion, the network formed by the base and the “moving” stations was calculated by fixing the positions of the two reference stations outside the flow. Calculations were carried out by using the precise orbits of the International Global Positioning System Service for Geodynamics (IGS) and by taking account of the models of variation of the phase center of the antennas recommended by the IGS. Given the very short distance between the stations, the calculations were carried out on the  $L1$  frequency

only (less noisy than  $L2$ ), without estimating tropospheric parameters, and 95% of the phase ambiguities were solved.

The final result is one baseline vector (north–south component (NS)= $X$ ; east–west component (EW)= $Y$ ;  $Z$  component = altitude) per observation session and

couple of stations. Thereafter, the primary interest is in the baseline vectors connecting the reference station MLZE and the “moving” stations. Calculations were carried out for sessions of 24, 12, 6, 3 and 1 h, in order to determine the accuracy variation as a function of the session duration.

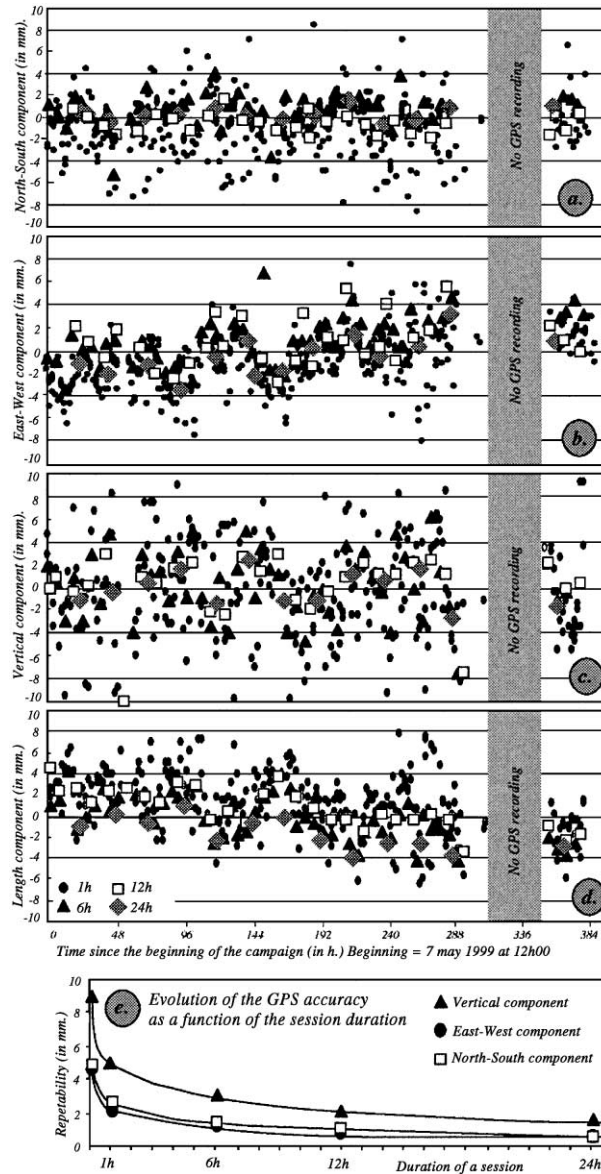


Fig. 3. Variation of the MLZE–PIL2 baseline for different calculations. N–S (a), E–W (b) and vertical (c) components, length variation (d) and repeatability on the components (e).

### 5.3. Measurements accuracy and optimal session duration

The component variations of the MLZE–PIL2 baseline (the two fixed stations) in May 1999 determine the real precision of the measurements. Fig. 3 shows the N–S (Fig. 3a), E–W (Fig. 3b) and vertical (Fig. 3c) components and the length variation (Fig. 3d) of this baseline, as a function of time, for sessions of 24-, 12-, 6- and 1-h durations. The two stations, 1.1 km apart, are located on open sites a priori free from multipath effects. The experimental accuracy is quantified by the quadratic weighted root mean square of the measurement scatter with respect to the weighted mean or repeatability (Dixon, 1991). The short-term repeatability is defined with respect to the average of the measurements weighted by their standard deviations, where the measured quantity  $m_i$  (which represents the N–S, E–W or vertical component) obey a law of the type  $m_i = m_0 + \varepsilon_i$ , where  $\varepsilon_i$  is a random variable of null average and variance  $\sigma_i^2$ . The long-term repeatability is defined with respect to a statistical model integrating a temporal evolution at a constant velocity ( $a$ ) of the type  $m_i = m_0 + at_i + \varepsilon_i$ . In both cases, the variances  $\sigma_i^2$  were obtained by propagating the a priori variances on the observations in the GPS data inversion process.

Fig. 3a–d clearly shows that the scatter increases when the session duration decreases. Fig. 3e shows the evolution of the accuracy in the three dimensions as a function of the session duration. For a baseline of 1.1-km and 1-h sessions, the short-term repeatability reaches 2.7, 2.2 and 5.0 mm, respectively, for the N–S, E–W and vertical components (Fig. 21). These results are consistent with the values obtained by Genrich and Bock (1992) and Pragnère (1996). Long-term repeatability reaches 2.5, 2.4 and 4.8 mm, respectively, for the same components. The maximum measurement scatter reaches (respectively for 24, 12, 6 and 1 h sessions) 3, 5, 6 and 8 mm on the N–S component, 3, 6, 6 and 9 mm on E–W component and 5, 5, 10 and 17 mm on the vertical component. A variance analysis enabled us to estimate the variance of all the measurements sessions, with the assumption that the scatters calculated over 3 weeks of measurements are good estimators of the scatter of all the measurements population. For 1-h sessions, the 95% confidence interval of the variance is 6–8.5 mm for the N–S and E–W components and 14.5–19.5

mm for the vertical component. For 24-h sessions, the 95% interval confidence of the variance is 1.5–3.5 mm for the N–S component, 2–3.5 mm for the E–W component and 4–6 mm for the vertical component.

These values give the detectability threshold for a significant motion and a given temporal resolution: between 3.5 mm/24 h and 8.5 mm/h in planimetry, between 6 mm/24 h and 19.5 mm/h in altimetry. The GPS is thus adapted to the measurement of low dynamic deformations. The measurement scatter observed, in particular for short sessions (high frequency noise), results from the variations of the satellite constellation and the multipath effects (Genrich and Bock, 1992; Galisson, 1998). Fig. 3b,d show, moreover, a length reduction of the baseline MLZE–PIL2, small but clearly identifiable, about 5 mm in 17 days. These variations are probably related to the instability of the slope where pillar PIL2 was established. This is why, subsequently, GPS displacements will only be analysed by the variations of the baselines connecting MLZE to the “moving” sites. Nevertheless, the movement of PIL2 is lower than the topometric measurement accuracy and the validation of the GPS measurements by topometry is efficient.

## 6. Analysis and interpretation of the results

### 6.1. GPS/extensometry/topometry validation

Fig. 4 shows the temporal evolution of the displacements of GPS “moving” sites COU1, COU2, COU3 and COU4. The general movement of the flow is clearly detected by the GPS measurements. The cumulated displacements (Fig. 4c,e) obtained in 17 days of continuous measurements vary between 0.15 (planimetry) and  $-0.01$  m (altimetry) at site COU1 and between 2.04 (planimetry) and  $-0.75$  m (altimetry) at site COU4. These displacements correspond to an average velocity of 0.9 mm/day at site COU1 and 12 cm/day at site COU4 (Fig. 4d). The white points in Fig. 4c,e show the results of the topometry measurements on targets located in the vicinity of the GPS sites. The displacements determined by GPS are conformable with those measured by topometry. The average variation is 0.8 cm for an intrinsic accuracy of the topometric measurements defined in Fig. 2c.

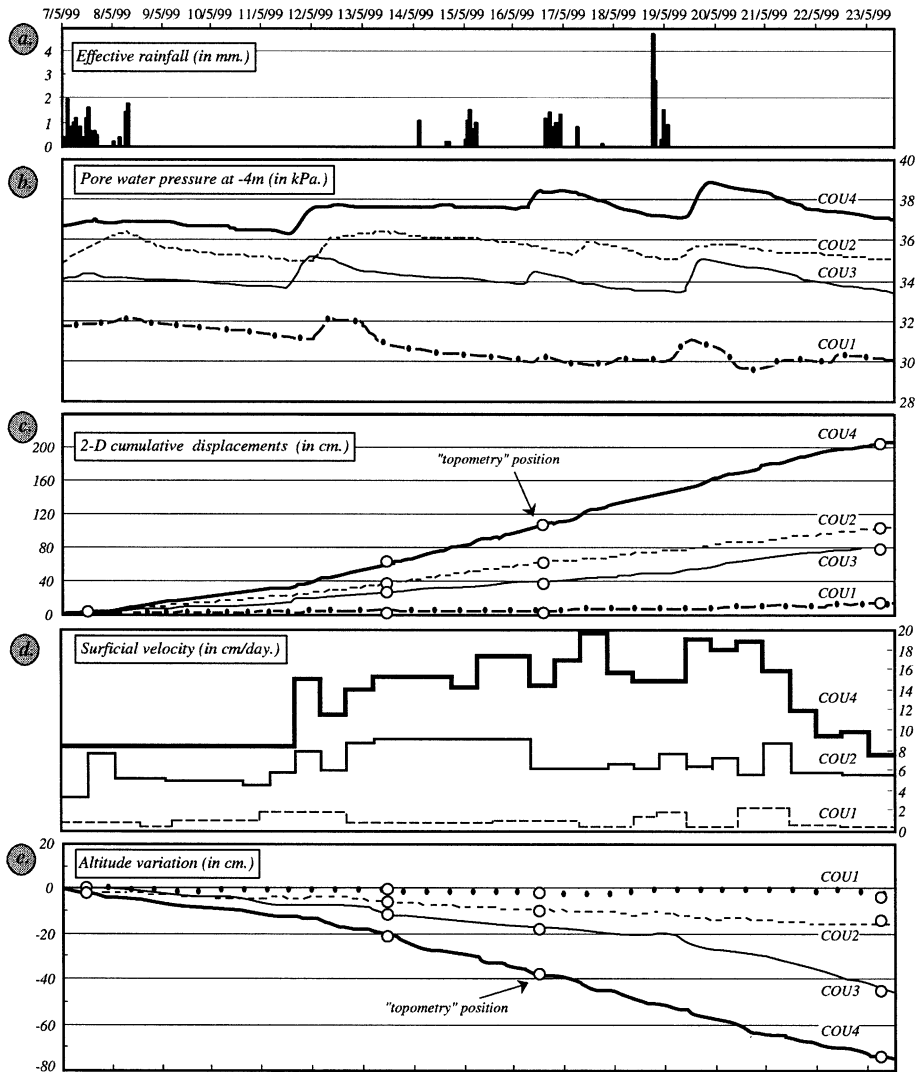


Fig. 4. Rainfall–GWT–displacements relationships for the GPS “moving” sites in May 1999. Effective rainfall (a), pore water pressures variations (b), cumulated planimetric displacements (c), surficial velocity variations (d) and cumulated altimetric displacements (e).

Fig. 5 shows the temporal evolution of the displacements of the extensometric “moving” site, between June 1999 (installation of the device) and November 1999 (removal of the device before snowfalls). The 3-D displacements reach 1.10 m with a succession of deceleration and acceleration periods related to the position of the GWT in relation to the rainfall. The velocity varies between  $<1$  and 9 cm/day in period of high GWT. The displacements measured by the unreeling of the wire coincide with the topometric control measurement; the average

variation on the calculation of the displacement vectors is  $\pm 1.1$  cm. Fig. 6 shows a zoom over the period of October 9–15, 1999 (period of displacements lower than 1 cm/day) where we have GPS, extensometric and topometric measurements of the same “moving” point. In 7 days, the GPS displacements (which result in the shortening of the baseline MLZE-COU4) reach 1.2 cm, the displacements measured by extensometry, 1.1 cm, the displacements measured by topometry, 0.95 cm. The slight variation of velocity (October 12, 1999) following an effective rain (net

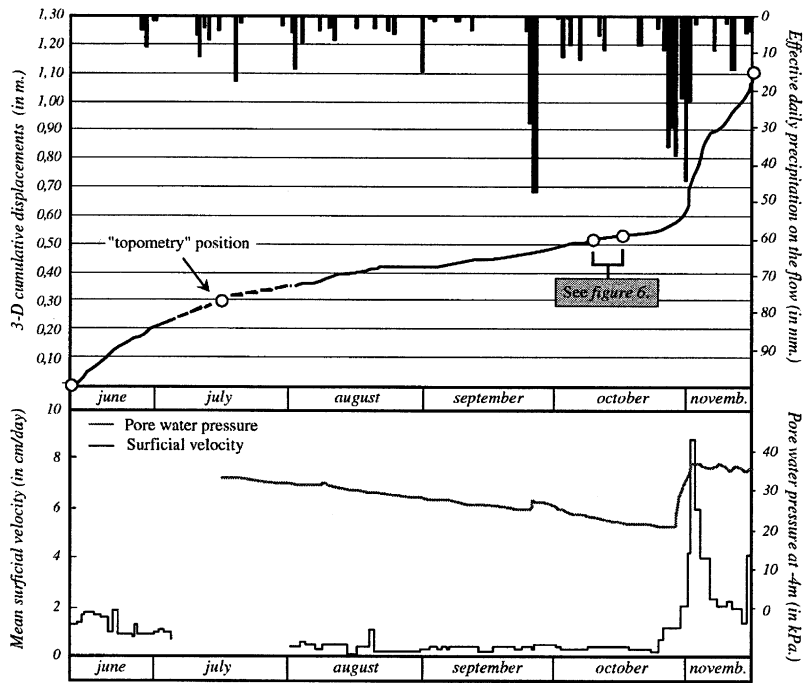


Fig. 5. Displacements measured by extensometry and topometry between June and November 1999.

rainfall minus potential evapotranspiration according to the Penmann formula) of 10 mm is significantly and simultaneously detected by the GPS and extensometric measurements. Thus, even for such velocity (0.2 cm/day), GPS detects, with an hourly temporal resolution, a significant movement in accordance with the classic surveying measurements. This velocity defines the lower movement detection limit by GPS and the extensometric device.

### 6.2. Spatialization of the displacements

The periodical topometric measurements, between July 1996 and November 1999, make it possible to quantify the amplitude and the velocity of the displacements and to highlight the partitioning of the flow in close connection to the paleotopography of crests and gullies (Flageollet et al., 2000). The general direction of the displacements is facing N-10° on the cross-

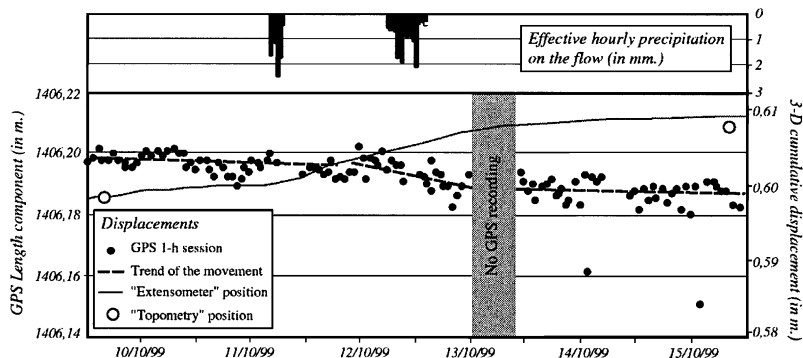


Fig. 6. Displacements measured by GPS, extensometry and topometry in October 1999.

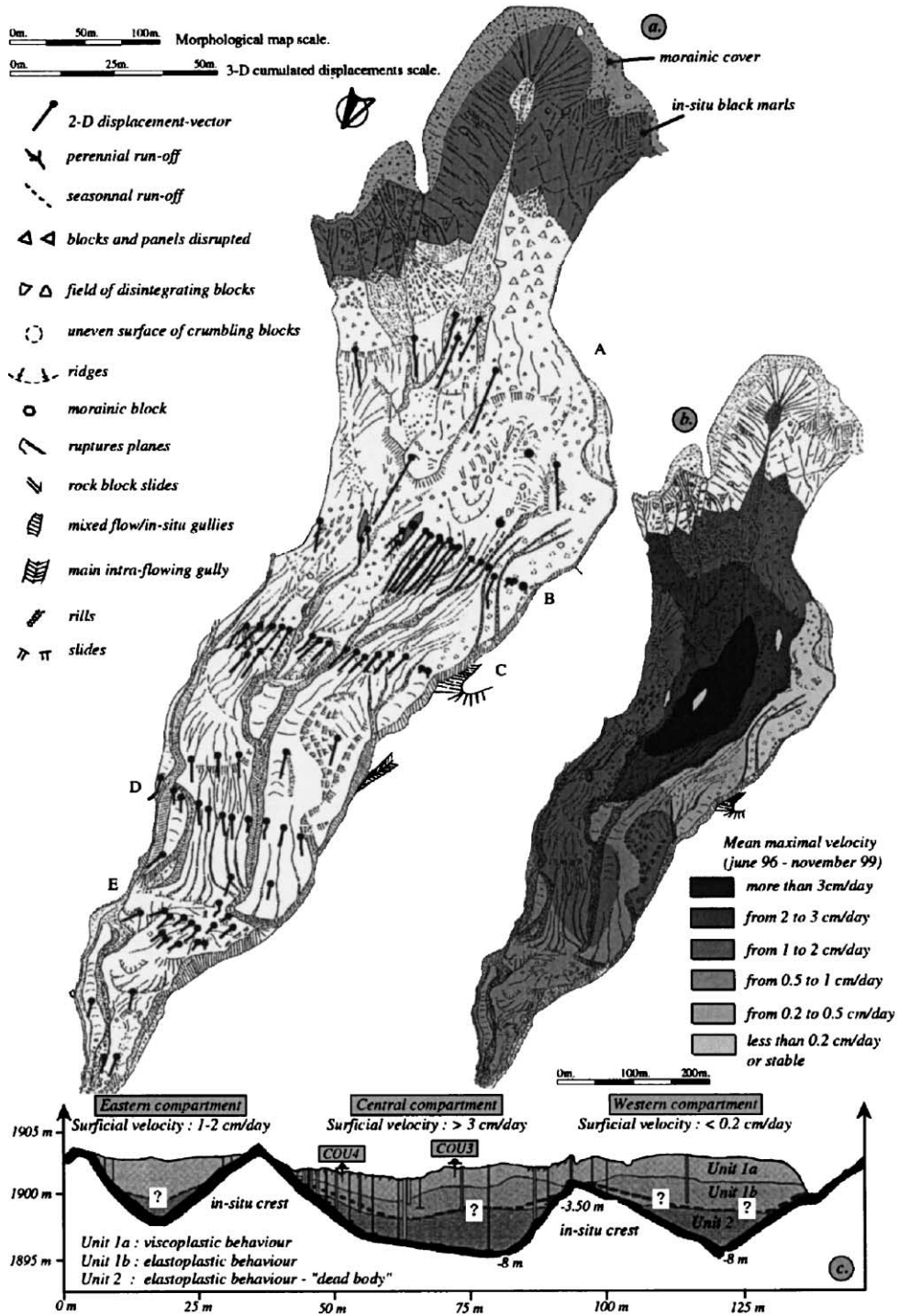


Fig. 7. Kinematics and mechanical behaviour of the Super-Sauze flow. Displacement vectors (a), maximal mean average velocities (b) and partitioning of the flow (c).

sections A, B, C and E and N-340° on the transect D and on the toe of the flow (Fig. 7a). It corresponds to the line of greatest slope and to the preferential axis of flow in the buried gullies. It thus underlines the layout of the flow. The targets located on the buried in situ crests are stable. One notices a reduction of the velocity downstream and from the axis to the flanks of the flow. The maximal observed displacements, between July 1996 and November 1999, reach (in planimetry) 24 m on the B cross-section, 19 m on the A cross-section, 11 m on the C cross-section, 5 m on the D cross-section and 3 m on the E cross-section (Fig. 8c), and range in altimetry (Fig. 8e) between  $-9.5$  (B) and  $-0.15$  m (E). The partitioning of the flow by the paleotopography appears as morphological evidence, in particular, among the A, B and C cross-sections (Fig. 7b), and in the axis of the flow (Flag-eollet et al., 2000) where the displacements are maximal. Water from the rainfall is channelled from the upper shelf under the A cross-section (limit of the depletion zone; Dikau et al., 1996), between two principal buried gullies (Fig. 7c): in the central compartment, the recorded maximal average velocities are higher than 3 cm/day, whereas they are lower than 0.25 cm/day in the western compartment drained laterally by the stream. Downstream of the C cross-section, the displacements decrease mainly because of the drainage by the intraflowing gully incised about 4–5 m.

### 6.3. Long-term temporal dynamic of the flow

Fig. 8 shows the cumulated planimetric (Fig. 8c) and altimetric (Fig. 8e) displacements and the mean average velocity (Fig. 8d) of the “fastest” targets for each cross-section in relation to hydroclimatic parameters (net and effective daily precipitation, index of antecedent effective precipitation, Fig. 8a; decade hydrologic net balance and pore water pressures—PWP—on the E cross-section, Fig. 8b) for the hydrologic years 1996–1997, 1997–1998 and 1998–1999. These curves enable us to establish the rainfall–GWT fluctuation–displacement relationships on an annual scale, and make it possible to identify the seasonal variations of the flow. Generally, the piezometric level variations are correlated with rainfall (Fig. 8b). The correlation is even more evident with the effective rainfall. The analysis of the piezometric behaviour shows a great amplitude of PWP variations (up to 20

kPa) with sudden recharge following to the snowmelt in spring or to unfavourable climatic periods (cumulated effective rainfall threshold of about 50–60 mm) in autumn. One notes the briefness of the episodes of high groundwater levels and a maximum PWP not exceeding 35 kPa for piezometers located at  $-4$  m below the ground surface (GS). Slow and progressive drainage takes place from June to September and during winter when snow covers the flow. The water level becomes lower each year, particularly during the hydrological year 1998–1999 when the hydrologic balance was in deficit (annual net rainfall less by 25% than the normal).

The long-term displacements in amplitude are directly controlled by the hydrological history of the site because the velocity peaks are localised in spring during the snowmelt (Fig. 8d), recharge events that is now necessary to analyse in detail.

### 6.4. Short-term and seasonal dynamic of the flow

The rainfall–GWT–displacements relationship can now be approached on the finer scale of rain events according to the continuous GPS and extensometric measurements. The comparison between the displacements measured by GPS on sites COU1 to COU4 in May 1999 (Fig. 4c) confirms the kinematics of the flow identified by the topometric survey. For this period, the GWT is in a high position (average position, respectively, on the B, C, and E cross-sections at  $-0.24$ ,  $-0.45$  and  $-0.85$  m/GS). By comparing the effective rainfall to the groundwater level fluctuations (Fig. 4a,b), one notes that certain rain events correspond a nonsimultaneous increase of the water level in all points of the flow. This “dephasing” is explained by the fact that the first rainfalls contribute to the melting of the snow, which still covers the flow on the B and C cross-sections at the beginning of the month. The simultaneous water level increase of May 11, 1999 corresponds to a period of strong insolation having accentuated the snowmelt.

On the B and C cross-sections, velocities are higher with velocity peaks which correspond to peaks of PWPs (Fig. 4b,d). GPS measurements highlight an identical behaviour of the whole “moving” points, namely that the velocities can be high (higher than 10 cm/day) as soon as the GWT is located near  $-0.30$  m/GS. PWP variations between the upper part and the

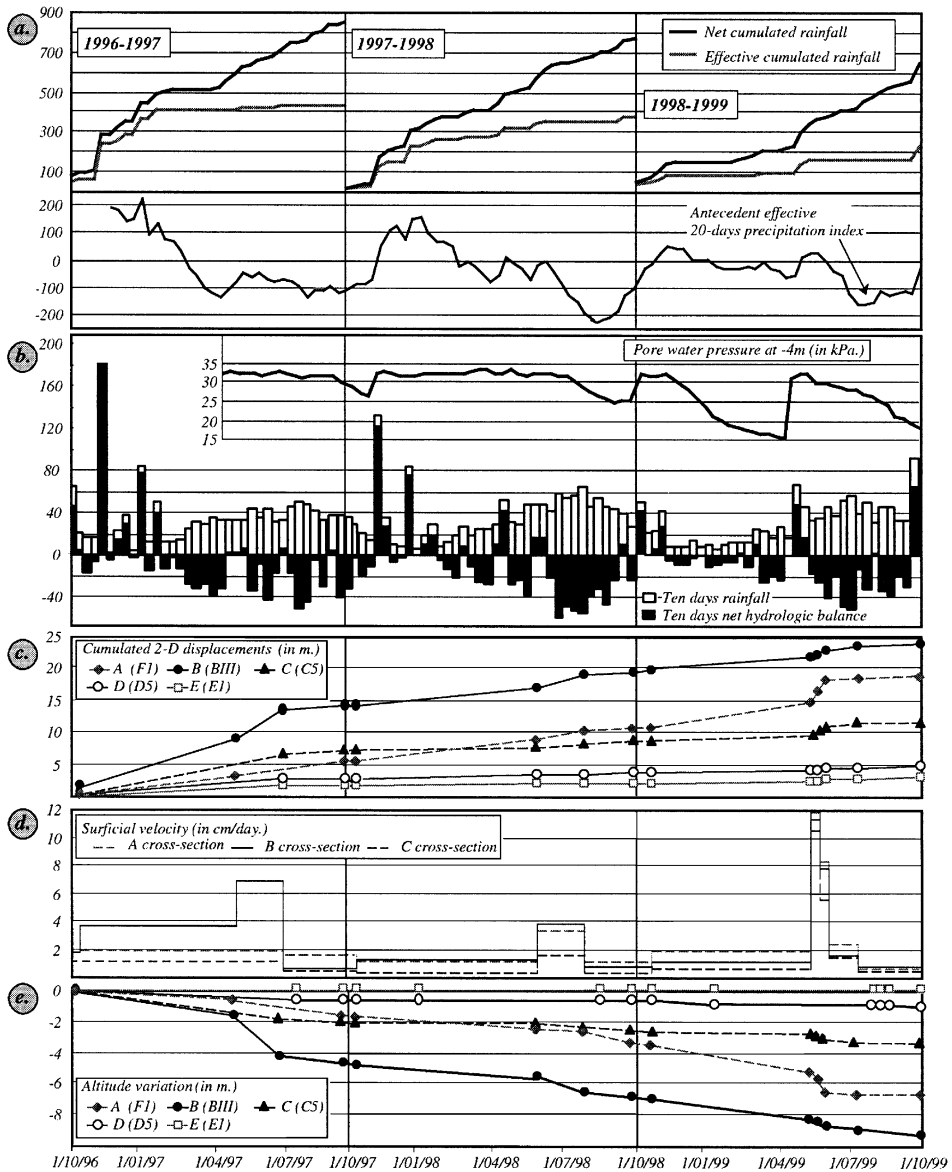


Fig. 8. Rainfall–GWT–displacements relationships between 1996 and 1999. Net and effective daily cumulated rainfall (a), hydrologic net balance and pore water pressures variations on the E cross-section (b), cumulated planimetric displacements (c), mean average surficial velocity (d) and cumulated altimetric displacements (e).

lower part of the flow partly control the velocity variations. Thus, on the B and C cross-sections, where the GWT is constantly fed by the snowmelt of the upper areas of the flow, the velocities vary between 6 and 20 cm/day, whereas they do not exceed 2 cm/day on the E cross-section. The role of the PWP's is

reinforced by the longitudinal slope (20° for site COU4, 15° for site COU2, 10° for site COU3 and 2° for site COU1), which accentuates the velocity differences under the action of gravity. The significant displacement differences between COU3 and COU4, separated by only about 30 m, is explained by a GWT

position in COU3 approximately 0.30 m lower than in COU4, by the variation of the longitudinal slope of the flow and by the influence of the paleotopography (COU4 on the flanks of an in situ crest, COU3 at the vertical of a quasi-flat sector; Fig. 7c) guiding the flow.

For site COU4 (Fig. 4d), the average velocity reaches 12 cm/day in May 1999 and only 0.2 cm/day in October 1999 (dry period; Fig. 6). This seasonal rhythm is directly due to GWT fluctuations in low position October (average position  $-2.10$  m below GS). For the greatest period of observation provided by the extensometric measurements (between June and November 1999), it is similar (Fig. 5): velocities fall from 2 cm/day at the end of spring to less than 1 cm/day during summer and autumn, in direct relationship to the drainage of the water table.

Effective rainfall of about 10 mm is enough during the general drainage and decreasing velocity period to produce a small piezometric level increase and a consequent acceleration. It is important to note that despite the significant drainage during summer, velocities do not cease and the material continues to flow solely under the influence of gravity.

The high cumulated rainfalls and snowfalls of October 1999 control the very fast recharge of the GWT, which reaches its level of spring in 5 days (Fig. 9a) and involves a sudden acceleration of the movements (Fig. 9b). If the accumulation continues, displacements increase and accelerate to a velocity peak quasi-simultaneous to the PWP peak. It is noted that those are not maintained at their highest values and drainage takes place more slowly than recharge, whereas the velocity decreases very quickly.

Continuous measurements appear here, and maybe more than elsewhere, essential to understand the dynamics of the flow and to fix PWP thresholds values. A sudden GWT loading involves acceleration of the flow. These are initiated (Fig. 9c) as soon as the water level ranges between  $-0.50$  and  $-0.40$  m below the ground surface (i.e. 35 kPa at  $-4$  m). In the same way, the velocity decreases gradually as soon as the level reduces to  $-0.80$  m below the topographic surface (i.e. 32 kPa at  $-4$  m). The relationship between PWP and velocity can be easily modelled by a hyperbolic regression with a determination coefficient of 0.92. The scatterplot is limited by an “envelope” curve delimiting PWP triggering thresholds on the acceleration of the movements.

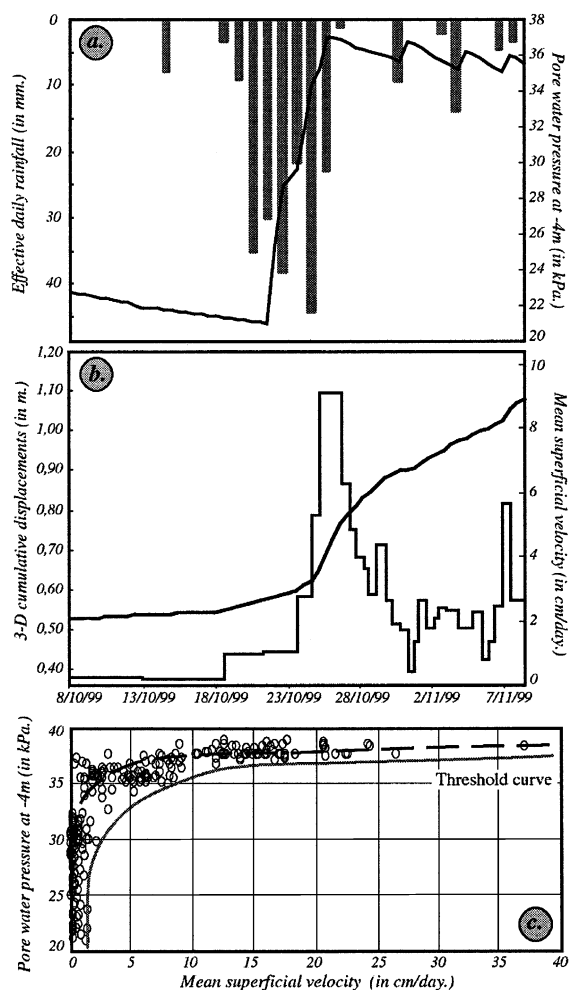


Fig. 9. GWT recharge and surficial velocity variations in October 1999. Effective daily rainfall and PWP variations (a), 3-D cumulated displacements and mean velocity (b) and PWP–velocity relationship (c).

For PWP highest to 35 kPa, accelerations occur with a velocity higher than 2–3 cm/day—the reached amplitude is thus a function of the interval of time where the water level remains above this threshold.

### 7. Discussion on GPS measurements: processing strategies and monitoring precautions

The GPS technique, as demonstrated, adapts perfectly to the periodic or continuous monitoring of

geophysical entities (volcanoes, glaciers, landslides) subject to some precautions, with a very good temporal resolution (hourly or even less if the movement is significantly fast), and can highlight transient phenomena not detectable (or with considerable difficulty) by traditional monitoring techniques. Thus, the detailed analysis of the time series MLZE–COU4 in October 1999 shows a particular behaviour (Fig. 10). Sessions of 1, 3 and 6 h indicate a periodic variation of 1 cm amplitude during the first 3 days of measurements. The fourth day is marked by a jump in the time series, particularly clear on the vertical component, followed by stabilisation of the movement the fifth and sixth days. The variations of the average hourly air temperature at the Super-Sauze weather station are clearly correlated with the displacements, with a dephasing of approximately 2 h. The fact that all of the sessions (1, 3 and 6 h) show this same behaviour (smoothed by the sessions of 12 and 24 h), the periodical character of these variations, their orders of magnitude higher than the precision of

the GPS measurements (1.9 mm in planimetry, 3.5 mm in altimetry; Fig. 3e) and their correlation with the air temperature variations argue in favour of a geophysical phenomenon (hydrothermal dilation? influence of the solar radiation?) and not of a bias in the GPS measurements. Nevertheless, this phenomenon had not been observed in May 1999, for identical daily thermal amplitudes (6 °C). The continuous survey by GPS highlights these “transient” phenomena. The latter can be determined in the forecast of the long-term movements, whereas they could be unnoticed with discrete measurements.

The interest of GPS lies in the possibility of continuous 3-D measurements of the displacements, with a millimetre-level accuracy and hourly resolution. Today, it is easy to find a GPS data acquisition device (receiver, antenna) for an equivalent price, maybe lower, to that of an automated geodetic station. For short baselines, the use of monofrequency receivers (less expensive) is sufficient to guarantee an infracentimetric accuracy. The cost/gain ratio for GPS monitoring is interesting for the survey of large features or the survey of entities where the morphological configuration is not adapted to optical measurements (inter-visibility). Indeed, compared to the latter, GPS makes it possible to be freed from the need of one (or several) stable site facing the landslides, as the GPS survey does not require a direct line of sight between the measurement sites. The “fixed” reference site can, for instance, be located in a neighbouring valley. Moreover, GPS measurements can be undertaken in any type of weather (rain, snow, fog, strong sun) and at night. The GPS offers a more homogeneous precision in the three dimensions than optical techniques. Last, but not least, the postprocessing of the code and phase data can be automated by computer scripts and thus carried out by a nonspecialist user.

If compared to the “traditional” monitoring techniques, GPS offers many advantages; nevertheless, it remains subjected to a lot of constraints common to all geodetic methods. It is necessary, for example: (i) to find a very good and long-term stable area to install the “fixed” survey points around the moving mass; these “nonmoving” points will be used as reference points for the quality check of the measurements; (ii) to install targets which are sufficiently anchored (minimum of 1 m) to translate the movement of a representative 1-m depth section of ground and not

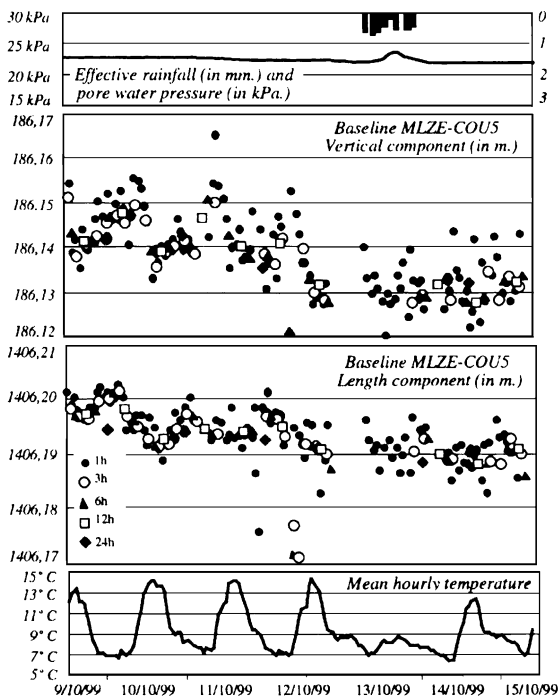


Fig. 10. MLZE–COU4 baseline in October 1999. Variation of the vertical and length components and evolution of the mean hourly temperature.

only of the surficial movements; (iii) that targets (in the case of tacheometry) or antennas (in the case of GPS) must be installed vertically as near as possible to the ground surface, 10 cm approximately, in order to limit the effects of the wind (oscillation). A constraint specific to GPS measurements lies in the obligation to ensure, for each site, a good sky visibility in all the directions (no masking by topography or forest) in order to permanently receive the signals emitted by at least four satellites. Let us add that, in the case of a continuous survey, to guarantee millimetre-level accuracy, the following precautions must be taken: the baseline must be less than 5 km and the GPS sites must be located at more or less the same altitude to minimise the potential errors due to different tropospheric delays.

Within the framework of a warning system, the advantage of the GPS technique over the traditional methods is also established in terms of productivity and precision. The mode of acquisition of the data and the possibility of sending them to a processing and decision center in quasi-real time makes it possible to optimise the device response time/forecast ratio. Moreover, GPS enables us to have, in a permanent way, upgraded day-to-day information directly “understandable” by the responsible authorities. Finally, GPS appears, subject to having a power supply or batteries effectively reloaded by solar panels, less consuming in term of maintenance than an extensometric device or an automated geodetic station. GPS measurements appear very easily adaptable to any type of geophysical entity.

## 8. Conclusion

The use of GPS on the Super-Sauze earthflow is a first attempt at the continuous measurements of the displacements of a landslide over a long period. These results could not have been obtained simultaneously in several points of the flow, easily and effectively, by the other traditional monitoring methods because of the very specific constraints of the site. In addition to those obtained before, these results have made it possible to quantify the 3-D kinematics of the flow and to highlight the rhythms of behaviour.

These first experiments were carried out on a number of points limited by the number of GPS

receivers available and the heavy logistics of their maintenance: GPS receivers used during this study were not completely optimised for this kind of application because of their significant consumption of energy and their relative low memory size. But these two points are now partly solved by the manufacturers. The results obtained are relevant to the traditional geodetic measurements. The study shows that it is possible, even for short sessions (1 h), to obtain an accuracy of a few millimetres on short baselines (<1 km), better than those obtained by tacheometry or extensometry. Moreover, the results show that GPS makes it possible to continuously follow the dynamics of geophysical entities with weak and slow displacements ( $\sim 5$  mm/day).

For the survey of landslides, GPS offers the advantage of delivering a three-dimensional positioning with an infracentimetric accuracy for 1-h sessions. This technique does not require a direct line of sight between the sites located on the moving mass and the reference sites. With a communication device to send data to a processing center, the same accuracy as that obtained here can be obtained in real-time, and the GPS can form part of a warning system. The use of GPS for this type of application is, however, limited by the environmental characteristics of the site (relief, vegetation), which can constitute potential masks limiting the sky visibility or create multipaths. In this case, the accuracy of the measurements is degraded more quickly when the duration of the sessions decreases (Galisson, 1998). The cost of the device and its maintenance are still obstacles at the present time for a routine application. However, the rapid technical progress combined with a diminution of the costs will facilitate their application in the long term.

## Acknowledgements

This program was financed by the CNRS within the framework of the INSU-PNRN contract 97/99-34MT. The GPS used came from INSU; Contribution INSU No. 269; Contribution Géosciences Azur No. 377. Thanks to S. Hartig, S. Klotz, S. Pierre, A. Puissant and A. Remaître for the help on the field. Very special thanks are due to C. Gerin for the reviewing of the English version of this article.

## References

- Angeli, M.C., Gasparetto, P., Menotti, R.M., Pasuto, A., Silvano, S., 1995. A system of monitoring and warning in a complex landslide in northeastern Italy. *Landslides News* 8, 12–15.
- Angeli, M.C., Pasuto, A., Silvano, S., 2000. A critical review of landslide monitoring experiences. *Engineering Geology* 55, 133–147.
- Ashkenazi, V., 1973. The measurements of spatial deformation by geodetic methods. 1st Symposium on Field Instrumentation in Geotechnical Engineering. British Geotechnical Engineers Society, London, pp. 124–156.
- Barbarella, M., Bitelli, G., Folloni, G., Gubellini, A., Russo, P., Tomassini, L., 1998. Deformation survey on landslides using terrestrial measurements and space techniques. Vth International Symposium on Deformation Measurements, Fredericton, Fédération Internationale des Géomètres, Geneva, pp. 195–201.
- Bromhead, E.N., Curtis, R.D., Shofield, W., 1988. Observations and adjustment of geodetic survey network for measurement of landslide movement. Vth International Symposium on Landslides, Lausanne, vol. 1. Balkema, Rotterdam, pp. 383–386.
- Brown, C.J., Karuma, R., Askhenazi, V., Roberts, G.W., Evans, R.A., 1999. Monitoring of structures using the GPS. Proceedings of the Institution of Civil Engineers, Structures and Buildings, vol. 134, pp. 97–105.
- Brunsdon, D., Prior, D.B., 1984. Slope Instability. Wiley, Chichester, 456 pp.
- Colas, G., Locat, J., 1993. Glissement et coulée de La Valette dans les Alpes de Haute-Provence: Présentation générale et modélisation de la coulée. Bulletin de Liaison des Laboratoires des Ponts et Chaussées 187, 19–28.
- Dikau, R., Brunsdon, D., Schrott, L., Ibsen, M.-L., 1996. Landslide Recognition: Identification, Movement and Causes. Wiley, Chichester, 251 pp.
- Dixon, T.H., 1991. The Global Positioning System. Review of Geophysics 29, 249–276.
- Engel, T., 1986. Nouvelles méthodes de mesure et d'analyse pour l'étude des mouvements de sol en terrains instables. PhD Thesis Ecole Polytechnique Fédérale de Lausanne (EPFL), 108 pp.
- EPFL, 1985a. Les travaux de mensuration en terrain instable. Projet d'école "Détection et Utilisation des Terrains Instables", DUTI. Ecole Polytechnique Fédérale de Lausanne (EPFL), 27 pp.
- EPFL, 1985b. Capteurs de Mesure et de Détection, 2nd edn. Ecole Polytechnique Fédérale de Lausanne (EPFL), Presses Polytechniques Romandes, Lausanne, 212 pp.
- Evrard, H., Léger, B., Spinnler, Y., 1990. Télésurveillance des falaises de l'autoroute A40. Revue Generale des Routes et Aéroports 680, 11–18.
- Fix, R.E., Burt, T.P., 1995. Global Positioning System: an effective way to map a small area or catchment. *Earth Surface Processes and Landforms* 20, 817–828.
- Flageollet, J.-C., Maquaire, O., Weber, D., 1998. New technologies for landslide hazard assessment in Europe. NEWTECH, Programme DG XII, Final Report, 431 pp.
- Flageollet, J.-C., Malet, J.-P., Maquaire, O., 2000. The 3-D structure of the Super-Sauze earthflow: a first stage towards modelling its behaviour. *Physics and Chemistry of the Earth (B)* 25, 785–791.
- Follacci, J.P., 1999. Seize ans de surveillance du glissement de La Clapière (Alpes-Maritimes). Bulletin de Liaison des Laboratoires des Ponts et Chaussées 220, 35–51.
- Fruneau, B., Achache, J., Delacourt, C., 1996. Observation and modelling of the Saint-Etienne-de-Tinée landslide using SAR interferometry. *Tectonophysics* 265, 181–190.
- Galissou, L., 1998. Utilisation du GPS de précision pour la mesure de faibles déformations du sol: Mémoire. DEA "Systèmes Spatiaux et Environnement". Université Louis Pasteur, Strasbourg, 109 pp.
- Genrich, J.F., Bock, Y., 1992. Rapid resolution of crustal motion at short ranges with Global Positioning System. *Journal of Geophysical Research* 96, 3261–3269.
- Gervaise, J., Mayoud, M., Beutler, G., Gurtner, W., 1985. Test of GPS in the CERN-LEP control network. In: Welsch, W.M., Lapine, L.A. (Eds.), Proceedings of the International Federation of Surveyors, Doppler and GPS Measurements for Engineering Surveys, Munich, A.A. Balkema, Rotterdam, pp. 337–358.
- Gili, J.A., Corominas, J., Rius, J., 2000. Using Global Positioning System techniques in landslide monitoring. *Engineering Geology* 55, 167–192.
- Girault, F., 1992. Auscultation de versant instables par imagerie numérique. Thèse Ingénieur CNAM, Paris, 193 pp.
- Gulla, G., Nicolletti, P.G., Sorriso-Valvo, M., 1988. A portable device for measuring displacements along fractures. Vth International Symposium on Landslides, Lausanne, vol. 1. Balkema, Rotterdam, pp. 423–426.
- Herring, T.A., 1996. The Global Positioning System. *Science America*, 32–38, February.
- Higgitt, D.L., Warburton, J., 1999. Applications of differential GPS in upland fluvial morphology. *Geomorphology* 29, 121–134.
- Hiura, H., Sassa, K., Fukuoka, H., 1996. Monitoring system of a crystalline schist-landslide: three dimensional displacement meters and underground erosion. VIIth International Symposium on Landslides, Trondheim, vol. 3. Balkema, Rotterdam, pp. 1141–1146.
- Hofmann-Wellenhof, B., Lichtenegger, H., Collins, J., 1997. GPS—Theory and Practice, 4th edn. Springer, Wien, 389 pp.
- Hudnut, K.W., Behr, J.A., 1998. Continuous GPS monitoring of structural deformation at Pacoima dam, California. *Seismological Research Letters* 69, 299–308.
- Jackson, M.E., Bodin, P.W., Savage, W.Z., Nel, E.M., 1996. Measurement of local horizontal velocities on the Slumgullion landslide using the Global Positioning System. *U.S. Geological Survey Bulletin* 2130, 93–95.
- Joass, G.G., 1993. Stability monitoring on the West Wall of the Muja open cut. In: Szwedzicki, T. (Ed.), *Geotechnical Instrumentation and Monitoring in Open Pit and Underground Mining*. Balkema, Rotterdam, pp. 283–291.
- Kimura, H., Yamaguchi, Y., 2000. Detection of landslide areas using satellite radar interferometry. *Photogrammetric Engineering and Remote Sensing* 66, 337–344.
- King, R.W., Bock, Y., 1995. Documentation for the Gamit GPS Analysis Software. Scripps Institution of Oceanography, University of California, San Diego.
- Klotz, S., 1999. Recherches sur les conditions d'évolution des marnes noires du glissement-coulée de Super-Sauze: Mémoi-

- re, DEA “Systèmes Spatiaux et Environnement”. Université Louis Pasteur, Strasbourg, 120 pp.
- Krauter, E., 1988. Applicability and usefulness of field measurements on unstable slopes. *Vth International Symposium on Landslides*, Lausanne, vol. 1. Balkema, Rotterdam, pp. 367–373.
- Laboratoire Central des Ponts et Chaussées (LCPC), 1994a. Surveillance des pentes instables. Guide Technique, LCPC, 125 pp.
- Laboratoire Central des Ponts et Chaussées (LCPC), 1994b. Télésurveillance des ouvrages d’art et des sites. Projet National ITELOS, LCPC, 442 pp.
- Larson, K.M., Agnew, D.C., 1991. Application of the Global Positioning System to crustal deformation measurement, 1. Precision and accuracy. *Journal of Geophysical Research* 96, 16547–16565.
- Leick, A., 1995. *GPS Satellite Surveying*. Wiley, New York, 256 pp.
- Malet, J.-P., Maquaire, O., Klotz, S., 2000. The Super-Sauze flowslide (Alpes-de-Haute-Provence, France): triggering mechanisms and behaviour. *VIIIth International Symposium on Landslides*, Cardiff, T. Telford, London, pp. 999–1006.
- Mao, A., Harrison, C.G.A., Dixon, T.H., 1999. Noise in GPS coordinate time series. *Journal of Geophysical Research* 104, 2796–2816.
- Maquaire, O., 1990. Les mouvements de terrain de la côte du Calvados. Recherche et prévention. Documents du BRGM No. 197, 431 pp.
- Maquaire, O., Levoy, F., 1987. La topométrie en géomorphologie dynamique. *Travaux du CREGEPE*, vol. 6. Caen University, pp. 25–45.
- Martin, B., Weber, D., 1996. Vitesses de déplacement des mouvements de terrain à Vars (Hautes-Alpes, France): le recours aux archives et à la topométrie. *Revue de Géographie Alpine* 2, 57–66.
- Mattioli, G.S., Dixon, T.H., Farina, F., Howell, E.S., Jansma, P.E., Smith, A.L., 1998. GPS measurements of surface deformation around Souffriere Hills Volcano, Montserrat, from October 95 to July 96. *Geophysical Research Letters* 25, 3417–3420.
- Mikkelsen, P.E., 1996. Field instrumentation. In: Turner, A.K., Schuster, R.L. (Eds.), *Landslides Investigation and Mitigation*, TRB Special Report 247. National Academy Press, Washington, DC, pp. 278–316.
- Miserez, A., 1984. Evaluation de l’ampleur des mouvements de sol d’un flanc de vallée dans les Alpes valaisannes (Suisse). Journée d’études: “Auscultation des ouvrages en terre et des terrains”. Ecole Nationale des Ponts et Chaussées, Paris, 11 pp.
- Miyazawa, K., Yoshizawa, N., Onozuka, R., Hisamatu, F., 2000. Analytic system for landslide by different time photogrammetry: presumption of underground slide surface by analysis of surface displacement data of Hachimantai Sumikawa landslide area. *Journal of the Japan Society of Photogrammetry and Remote Sensing* 39, 39–47.
- Mohr, J.J., Reeh, N., Madsen, S.N., 1998. Three dimensional glacial flow and surface elevation measured with radar interferometry. *Nature* 391 (6664), 273–276.
- Newmann, A., Stein, S., Weber, J., Engeln, J., Mao, A., Dixon, T., 1999. Slow deformation and lower seismic hazard at the new Madrid seismic zone. *Science* 284 (5414), 619–621.
- Oka, N., 1988. Applications of photogrammetry to the field observation of failed slopes. *Engineering Geology* 50, 85–100.
- Peler, Y., Kahle, H.G., Cocard, M., Veis, G., Felekis, S., Paradissis, D., 1998. Establishment of a continuous GPS network across the Kefalonia fault zone, Ionian Islands, Greece. *Tectonophysics* 294, 253–260.
- Pingue, F., Troise, C., DeLuca, G., Grassi, V., Scorpa, R., 1998. Geodetic monitoring of Mt. Vesuvius Volcano, Italy, based on EDM and GPS surveys. *Journal of Volcanology and Geothermal Research* 82 (1–4), 151–160.
- Powers, P.S., Chiarle, M., 1996. A digital photogrammetric method to measure horizontal surficial movements on the Slumgullion landslide, Hinsdale County, Colorado. *U.S. Geological Survey Bulletin* 2130, 51–55.
- Pragnère, A., 1996. Optimisation des paramètres dans le traitement des données GPS d’une courte ligne de base (1.37 km). Rapport de Stage, Géosciences Azur, 15 pp.
- Rochet, L., 1992. Auscultation–Diagnostic–Surveillance. *Bulletin of the International Association of Engineering Geology* 45, 43–57.
- Röthlisberger, H., Aellen, M., 1970. Bewegungsregistrierung an des Zunge des Sietogletschers. *Schweizerische Bauzeitung* 88 (Jahrgang 43), 33–36.
- Sassa, K., 1984. Monitoring of a crystalline schist landslide: compressive creep affected by “underground erosion”. *Proceedings of the IVth International Symposium on Landslides*, Toronto, vol. 1. A.A. Balkema, Rotterdam, pp. 356–360.
- Schlemmer, H., 1982. Drahttextensometer zur Registrierung von horizontalen Bodenbewegungen über grössere Entfernungen. *Amtliche Vermessungs Nachrichten* 1, 2–21.
- Schmutz, M., Guérin, R., Maquaire, O., Desclôîtres, M., Schott, J.-J., Albouy, Y., 1999. Apport de l’association des méthodes TDEM et électrique pour la connaissance de la structure du glissement-coulée de Super-Sauze. *Comptes Rendus de l’Académie des Sciences* 328, 797–800.
- Sheperd, J.B., Herd, R.A., Jackson, P., Watts, R., 1998. Ground deformation measurements on the Souffriere Hills Volcano, Montserrat: II. Rapid static GPS measurements June 96–June 97. *Geophysical Research Letters* 25, 3413–3416.
- Singhroy, V., 1998. Landslide characterisation in Canada using interferometric SAR and combined SAR and TM images. *Advances in Space Research* 21, 465–476.
- Sjoberg, L.E., Pan, M., Asenjo, E., Erlingsson, S., 2000. Glacial rebound near Vatnajökull, Iceland, studied by GPS campaigns in 92 and 96. *Journal of Geodynamics* 29, 63–70.
- Theakstone, W.H., Jacobsen, F.M., Knudsen, N.T., 1999. Changes of snow cover thickness measured by conventional mass balance methods and by Global Positioning System surveying. *Geografiska Annaler* 81A, 767–776.
- Van Beurden, S., 1997. Hydrology, soil mechanics and kinematics of slow mass movements in the Widenbach catchment, Switzerland. PhD thesis, University of Utrecht, Netherlands, 253 pp.
- Varnes, D.J., Smith, W.K., Savage, W.Z., Powers, P.S., 1996. Deformation and control surveys: Slumgullion landslide. *U.S. Geological Survey Bulletin* 2130, 43–49.
- Weber, D., 2001. Contribution de la géomorphologie à la connais-

- sance des mouvements des terrains dans les “Terres Noires” alpines: le glissement-coulée de Super-Sauze (Alpes-de-Haute-Provence, France). PhD Thesis, Université Louis Pasteur, Strasbourg, 311 pp.
- Weber, D., Herrmann, A., 2000. Reconstitution de l'évolution géomorphologique de versants instables par photogrammétrie numérique: l'exemple du glissement de terrain de Super-Sauze (Alpes-de-Haute-Provence, France). *Bulletin Societe Geologique de France* 171, 637–648.
- Zhang, J., Bock, Y., Johnson, H., Fang, P., Williams, S., Genrich, J., Wdowinski, J., Behr, J., 1997. Southern California Permanent GPS geodetic array: error analysis of daily position estimates and site velocities. *Journal of Geophysical Research* 102, 18038–18055.